Grzegorz ŻYWICA
Tomasz Z. KACZMARCZYK

EXPERIMENTAL EVALUATION OF THE DYNAMIC PROPERTIES OF AN ENERGY MICROTURBINE WITH DEFECTS IN THE ROTATING SYSTEM

EKSPERYMENTALNA OCENA WŁAŚCIWOŚCI DYNAMICZNYCH MIKROTURBINY ENERGETYCZNEJ W OBECNOŚCI DEFEKTÓW UKŁADU WIRUJĄCEGO*

Today's energy systems increasingly use various types of microturbines to produce electricity. A specific feature of such machines is a high-speed rotor, whose rotational speed can be higher than 100,000 rpm. Failure-free operation of high-speed microturbine rotors requires both special design and high precision during the manufacturing process. What is more, proper procedures must be followed during run-up and coast-down phases; and also, dedicated diagnostic systems have to be used. This article discusses the experimental research conducted on a 2.5 kW vapour microturbine that operated in a prototypical combined heat and power plant. A series of measurements was carried out to evaluate the dynamic performance of the machine during normal operation. After the appearance of certain defects in the rotating system, it was necessary to perform a new series of measurements in order to assess the dynamic properties of the machine. The measurements results obtained in the form of vibration velocity spectrums made it possible to define diagnostic symptoms corresponding to particular defects. Similar diagnostic symptoms can occur during the operation of this class of turbomachines.

Keywords: *microturbines, high-speed rotors, damage in a rotating system, vibrations of turbomachines, rotor dynamics.*

We współczesnych systemach energetycznych coraz częściej do wytwarzania energii elektrycznej stosowane są różnego typu mikroturbiny. Charakterystyczną cechą takich maszyn są wysokoobrotowe wirniki, których prędkości obrotowe mogą przekraczać nawet 100 000 obr/min. Praca wirnika w takich warunkach wymaga zastosowania specjalnych rozwiązań konstrukcyjnych i bardzo dużej precyzji wykonania, a podczas eksploatacji zachowania odpowiednich procedur przy rozruchu i odstawieniu, a także stosowania dedykowanych systemów diagnostycznych. W niniejszym artykule zostały omówione badania eksperymentalne mikroturbiny parowej o mocy 2,5 kW, pracującej w prototypowym układzie kogeneracyjnym. Wykonane pomiary obejmowały ocenę stanu dynamicznego podczas normalnej pracy maszyny oraz badania jej właściwości dynamicznych w obecności defektów układu wirującego. Uzyskane wyniki pomiarów, w postaci rozkładów częstotliwościowych drgań, pozwalają na zdefiniowanie symptomów diagnostycznych typowych dla różnych defektów, które mogą pojawić się podczas eksploatacji tej klasy maszyn wirnikowych.

Słowa kluczowe: *mikroturbiny, wysokoobrotowe wirniki, uszkodzenia układu wirującego, drgania maszyn wirnikowych, dynamika wirników.*

1. Introduction

In modern electric power systems, distributed energy sources are playing an increasingly important role because these systems allow to efficiently produce thermal and electrical energy on a small scale from locally-available resources [3]. Depending on the available source of primary or renewable energy and energy demand, different types of thermal microturbines can be used to generate electricity [21]. Their basic features are as follows: power can be adapted to meet customer requirements, high operational availability (they can be switched on and off quickly compared to high-power steam turbines), small dimensions, high-speed rotors, high mobility, relatively low capital and operating costs [11]. All of these features are causing microturbines to be increasingly used, making a major contribution to the development of micro-power cogeneration systems [12].

The term 'microturbine' generally refers to a turbine whose electric power does not exceed 1 MW. Microturbines can be divided into several groups depending on their principle of operation, fluid flow

system design, power capacity, fuel type, or application. With regard to thermal microturbines, the main division is into gas and vapour microturbines. The rotors of gas microturbines are powered by exhaust gases from the combustor [2, 21]. Natural gas, biogas or kerosene can be used as fuel in gas microturbines. As for vapour microturbines, their rotors are powered by the vapour of the working medium, which circulates in a closed cycle and is heated using an external heat source [12]. In such a system, the following types of heat sources can be applied: gas or biomass boiler, geothermal source, solar collectors and waste heat from various production processes [7, 18]. The highest efficiency and profitability of installations with gas or vapour microturbines can be reached when the cogeneration is running (that is when there is a demand for both electric energy and thermal energy). Vapour microturbines have lower operating temperatures than gas microturbines and can produce electricity from low-temperature heat sources. Unlike gas mi-

croturbines, the operation of vapour microturbines does not depend on the fuel used because they are powered by working mediums that are not present in the combustion chamber. Steam turbines use water as their working medium. For vapour microturbines, various low-boiling mediums [6] are used. A thermodynamic cycle with a low-boiling medium is called the organic Rankine cycle (ORC).

High-speed rotors are used in energy microturbines. Shafts that rotate at high rotational speeds (which may exceed 100,000 rpm [13]) need to be supported by advanced and unconventional bearings such as magnetic [15], foil [28] and gas [19] bearings or even bearings lubricated with low-boiling mediums [14]. In addition to a good dynamic performance of the rotor over a wide rotational speed range, the bearing systems must be of great durability and reliability [7], allowing microturbines to operate without constant technical supervision. With the compact dimensions and low power output of microturbines, no strict procedures have to be followed every time they are set in motion as opposed to big power-station turbines [5]. As microturbine blades are small and rigid, they do not suffer from dynamic problems generally encountered in turbomachines used in the power industry [16]. However, microturbines can cause other dynamic problems that can result, among other things, from high rotational speeds, a wide range of operating speeds, lightness and low stiffness of the casings or their supporting structures being light and not rigid enough. Some low-boiling mediums used in ORC systems may exert a negative effect on microturbine subassemblies if the construction materials used (for example, plastics or elastomers) are not chemically resistant to these mediums. Since low-boiling working mediums are not so widely used as water, microturbine designers do not always have sufficient knowledge of their chemical compatibility with various materials.

Energy microturbines have only become popular in the past few years. In the past, they were scarce and only a few large international companies were involved in their production and research. Therefore, the scientific literature contains little information on construction details or guidelines for the operation of this type of machines. In fact, the results of research on the dynamic properties of microturbines operating under various conditions are almost nowhere to be found. Whereas, for those people who are engaged in the operation and maintenance of fluid-flow machines, such results are a valuable source of information that can be useful in developing a reliable diagnostic system, establishing alert and warning thresholds or for scheduling periodical inspections. The results of vibration measurements of fluid-flow machines make it possible to make structural changes to these machines or their support systems, which can lead to an improvement in their dynamic performance.

It is quite common for large steam turbines to be the subject of research for both scientists and engineers who are involved in the construction and operation of turbomachines. Therefore, there are many articles that present the results of research carried out not only on properly functioning machines but also on malfunctioning ones, where various types of defects are analysed. The experimental research of a 15 MW auxiliary steam turbine is presented in paper [22]. In this case, fractures occurred in the lacing wires that were mounted on the blades to reduce the displacement during their vibration. These fractures were observed in one of the stages located in the low-pressure part of the turbine. Both vibration measurements and experimental modal analysis of the blade were performed to identify the causes of the failure. The numerical analysis was performed as well. Its results are proof that there is a place on the blade in which the stress concentration occurred, which led to the failure. Article [27] also discusses a blade failure that occurred in the low-pressure stage of a 310 MW steam turbine. In this case, stress-corrosion cracking caused the failure. The authors analysed the microstructure of the blade material and concluded that some blades had not been properly tempered. An investigation of the rotor failure of a 60 MW turbine installed in a thermal power plant is discussed in article [1]. A fatigue crack of the shaft appeared after 10 years of operation. The authors of the article applied various diagnostic techniques to detect it, but the main focus was on investigating the fatigue fracture and performing material analyses. Paper [17] discusses torsional vibration and fatigue wear of the shaft of a 660 MW steam turbine. Two methods were considered to repair abrasion defects. A stress concentration occurred in the place where the wear defects are the most visible. An analysis of the impact of temperature changes on fatigue failures of the rotor of a steam turbine with a power of 1000 W is presented in article [24]. Poursaeidi et al. [23] determined temperature distribution on the gas turbine's casing and then analysed its effect on distortions and stress concentrations. An analysis, using an FEM model, was performed for the following power levels: 82, 87 and 96 MW. The results of temperature measurements performed on the real object were used during the creation of the model. Cracks that occurred in the immediate vicinity of certain holes in the casing were related to thermal stress concentrations. Article [25] exemplifies the practical application of the finite element method in an analysis of the causes of cracks in the casing of a helicopter engine. Mechanical and heat loads were taken into account in the analysis. In this case, cracks also occurred in places where the greatest concentrations of thermal stress were observed. In the opinion of the authors, the rotor vibrations had a negative effect on the fatigue life of the casing. The results of the vibration measurements of four large turbomachines (namely, centrifugal fans), both in steady and unsteady states, are presented in paper [4]. The research was carried out during a regular operation, which made it possible to identify the causes of the increased vibration level. The excessive vibrations were due, among other things, to an excessive unbalance of the rotating system, and also due to the fact that the inlet valves were not adjusted correctly. In the case of a large steam turbine, it would be reckless to conduct experimental research on a rotating system if we are fully aware that at least one of its elements is damaged because, under such conditions, a major failure could occur, which could pose a threat to people's lives and health. Therefore, the scientific literature lacks articles that present results of such types of experiments. In fact, various types of numerical models are commonly used to perform failure analyses of large turbines.

As far as the articles on energy microturbines are concerned, most of the experimental research presented in them mainly concern measurements of power, rotational speed and various thermodynamic parameters. Much less attention has been paid to vibration measurements and the study of different types of defects that may occur during operation. Conference paper [10] discusses a diagnostic system applied to a cogeneration system with a 95 kW gas microturbine. The diagnostic system was able to detect defects of the cogeneration system and malfunctions of the measuring system based on the values of the following parameters: thermal/electric power, thermodynamic parameters at the microturbine outlet and rotational speed of the rotor (which reached 70,000 rpm). However, no vibrodiagnostic parameters were measured by this system. Article [26] presents studies related to the dynamic characteristics of the high-speed rotor (30,000 rpm) of a microturbine with a complex geometry of the blade system. It was designed to be applied in a 100 kW gas microturbine. A test rig was built to perform experiments on the rotor. Ceramic rolling bearings were mounted on the test rig to support the rotor. Besides the results of the experimental research, the article presents a numerical model of the rotor, into which the substitute stiffness coefficients of the bearings were incorporated. The model allowed to perform a thorough analysis of the dynamic and thermal properties. The rotor vibration at low speeds was very low due to the high critical speed, which translated into the reliable operation of the machine. Hong et al. presented their research on the dynamic performance of the rotor of a 500 W gas microturbine, whose nominal speed is 100,000 rpm [8]. Numerical and experimental studies were conducted under different levels of the rotor unbalance. Additionally, a numerical model was developed,

which was used to perform a forced vibration analysis of the rotor.

The results of experimental studies on energy microturbines, which have been published so far in the literature, very rarely relate to vibration measurements. The authors of this article have not found any publications that present results of vibration measurements of this type of turbomachines, obtained in the event of malfunction or operation after some defects were detected. As a matter of fact, microturbines offer many possibilities in terms of active diagnostic experiments. Their downtimes do not lead to significant financial losses and, thanks to low production costs, they can undergo various modifications and the fast replacement of parts is not a problem. Although their rotors spin at high speeds, their low mass and compact dimensions make it possible to apply totally reliable protections to ensure the safety of experiments. Compared to large energy turbines, microturbines allow for many possibilities to conduct research (also where there are different defects).

The further part of the article focuses on the diagnostic research of a 2.5 kW ORC vapour microturbine. Vibration measurements were carried out in the presence of various types of defects in the rotating system, which occurred during operation. Even though vibrodiagnostic studies of this microturbine have been already presented in article [9], neither the dynamic problems nor the symptoms indicating the appearance of defects were detected at that time. Therefore, the results of previous studies should be treated as basis results, which can be referred to in case of changes in vibration characteristics. Damage, which occurred after the microturbine had been in operation for some time, has brought about new operating characteristics that can be analysed and different types of defects can be detected at the early stages of their development. This opens up new research possibilities in the field of maintenance and damage prevention when the machine is in service.

2. Characteristics of the microturbine

The tested microturbine was developed to produce electric energy in a micro-power ORC cogeneration system [29]. This is a prototypical machine designed within the framework of project No. POIG.01.01.02-00-016/08 (at the Institute of Fluid Flow Machinery of the Polish Academy of Sciences in Gdańsk), in cooperation with the Institute of Turbomachinery, Lodz University of Technology. The maximum thermal and electrical power of the cogeneration system was adapted to meet the average demand of residents of single-family houses. By using a boiler with a thermal power of approximately 25 kW, the microturbine is able to produce electric power of up to 2.5 kW. The microturbine with a generator is small in size due to its target use. The casing has a length of about 350 mm and an outer diameter of less than 200 mm. The sectional view of the microturbine, with its marked main parts, is shown in Fig. 1. In this figure, we can see how the rotor is placed inside the casing and how the bearings are arranged. The shaft is supported by two radial-axial gas bearings, constantly powered by the vapour of HFE-7100, which is the low-boiling working medium that also powers the fluid flow system of the microturbine. Thanks to the use of gas bearings, oil is not necessary for their lubrication and the rotor can reach very high rotational speeds with minimal friction losses in the bearing nodes. Since the bearing lubricant comes from the ORC, no additional lubrication system is required. There is also no possibility for the oil to mix with the low-
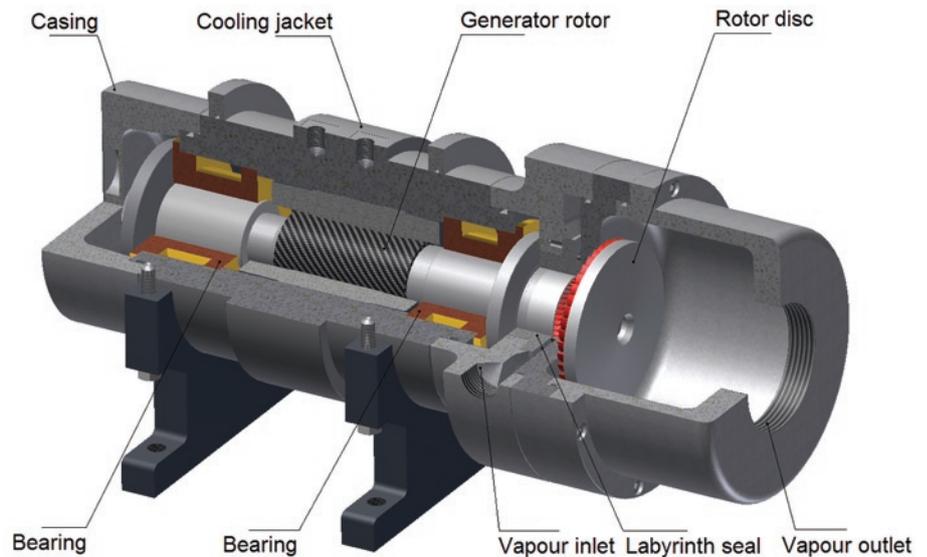
Fig. 1. The sectional view of the microturbine with its marked main parts

boiling medium. Microturbines that have this type of design are called oil-free microturbines.

The microturbine's fluid flow system consists of four turbine stages (two centripetal and two centrifugal). Thanks to this, it was possible to minimise the axial force that acts on the thrust bearings. The pressure and temperature of the low-boiling medium at the microturbine inlet is about 11 bar and 180°C, respectively. The nominal rotational speed of the rotor is 24,000 rpm; however, this machine is also adapted to constant operation at lower speeds. The sleeve of the synchronous generator is placed on the shaft of the microturbine, between the journals of the bearings. The generator stator is placed inside the casing, which is equipped with a cooling jacket. A non-contact labyrinth seal separates the microturbine's blade system from the generator and bearings. Since the same working medium is present in both parts of the casing, it was not necessary to use hermetic rotary seals. In this case, minor leaks inside the casing are acceptable and any surplus of the low-boiling liquid is removed by a system of holes. A photo of the entire microturbine, mounted on the test rig, is shown in Fig. 2. Compared to the model presented in Fig. 1, we can see additional rings connected by three threaded rods, which are used as an
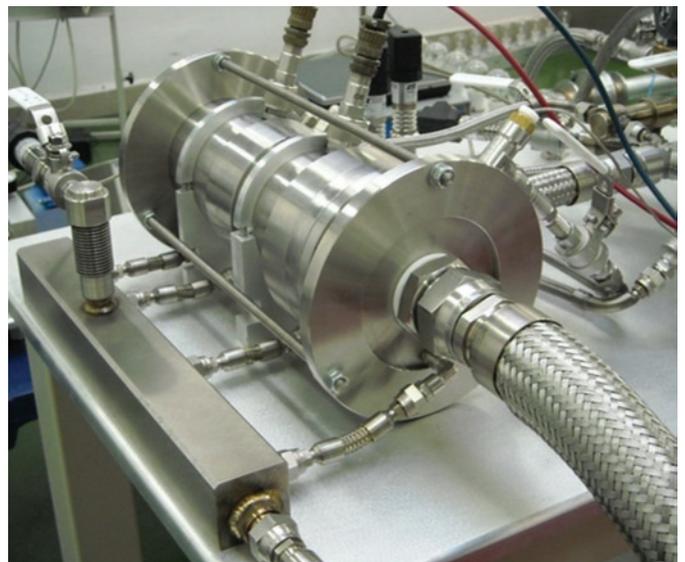
Fig. 2. The microturbine mounted on the test rig

extra measure of protection. The rotor was fitted inside the casing in the axial direction, before mounting the casing covers, the rotor disc and the thrust bearing keep plate. The microturbine was firstly tested using compressed air as a working medium and then tested in the ORC system where a low-boiling medium was present. It was possible, among other things, to check the correct operation of the rotating system, test the measuring system and check the casing for leakage.

Different types of internal and external loads act on particular elements of the microturbine during its operation. The centrifugal force, which results from the high rotational speed, acts on the entire rotating system (including the shaft, the rotor of the generator and the microturbine rotor disc). The residual unbalance of these components causes the rotor to vibrate in the radial and axial direction. Vibrations of the rotor may also be induced by natural vibrations of the rotor disc and blades. When the working medium's hot vapour comes into contact with the microturbine blades, it heats the rotor disc, shaft and casing. Vapour is also delivered to the gas bearings and contributes to the creation of thermal stresses. The vapour flowing through the blade system also causes vibrations of the entire shaft in the radial and axial direction. The operation of the electric generator inherently leads to heat accumulation in the confined space, which results in an increase in the temperature of the shaft, the casing and the generator alone. Since the operating temperature of the generator should not be too high, a water jacket is used for cooling. However, this causes an increase in the temperature gradient and additionally increases thermal stresses in the casing. In addition, these changes in temperature cause thermal deformations of the rotor and casing, which can lead to geometrical incompatibilities and leaks. Electric loads, resulting from the appearance of electromagnetic forces, act on the generator as well. All the loads of the rotating shaft are transmitted to the bearings by the journals. To operate properly, the microturbine's gas bearings require constant lubrication with the low-boiling medium's vapour. In fact, fluid friction in the bearings not only reduces friction losses but also prevents damage to the sliding surfaces. It is of utmost importance that bearings ensure stable operation of the rotor; at the same time, the vibration level should be as low as possible. This is particularly important in the case of high rotational speeds where rotor loads are higher and the lubricant flow can cause unstable bearing operation. All parts located inside the casing are exposed to the low-boiling medium, which is very penetrating and can have a destructive effect on some materials.

According to the above considerations, the microturbine components must be resistant to harsh operating conditions. Therefore, machines of this type require the application of advanced diagnostic methods and systems, which allow constant monitoring of their operating parameters. The results of previous numerical simulations show that changes in some parameters of the microturbine's rotating system discussed here can have a huge impact on the dynamic properties [30]. The same conclusion can be drawn with respect to the experimental research presented in the next part of the article.

3. Experimental studies of vibrations of the microturbine

3.1. Studies of the defect-free microturbine

Experimental studies of the microturbine were carried out in the IMP PAN laboratory, on the test rig that makes it possible to simulate real operating conditions. During the studies, the microturbine blade system and bearings were powered with vapour from the working medium (HFE-7100), at a maximum pressure and temperature of about 11 bar and 180°C, respectively. The values of these parameters are typical operating conditions for micro-power ORC cogeneration systems with multi-fuel boilers. In addition to the vibrodiagnostic measurements, the following operating parameters were measured: ther-

modynamic parameters of the working medium, rotational speed of the rotor, electric power of the generator. For vibration measurements, a portable vibration analyzer DIAMOND401A (XT version, produced by MBJ Electronics) and a uniaxial accelerometer (model 622B01, produced by PCB Piezotronics) were used. The accelerometer was mounted on the microturbine casing (using a magnetic holder), near the bearing located between the rotor disc and the generator (Fig. 1). Since the casing is made of stainless steel, sensors were fixed using additional stands made of ferromagnetic steel. The vibration level was measured at various locations on the casing in order to choose the appropriate location for the measuring point. The highest vibration level was recorded in the vertical direction, in the vicinity of the bearing situated near the rotor disc, and was considered the most relevant. A computer workstation with the MBJLab software (designed to allow users to diagnose the vibration of various types of machines, including rotating machines) was used for the analysis and visualisation of the measured results.

The results of vibration measurements were presented in the form of vibration velocity spectrums, which greatly facilitated their interpretation. As the maximum rotational speed of the tested machine was as high as 24,000 rpm (400 Hz), the measurements were made in a relatively wide frequency range, from 1 Hz to 800 Hz. A resolution of 1 Hz was used, which is the highest possible resolution of the vibration analyzer mentioned above. The spectral graphs presented in the article are the average results of three consecutive measurements, calculated using the RMS algorithm. To facilitate the comparison of the measured results with each other, the same maximum value (1 mm/s) occurs on the axes of ordinates (representing the RMS vibration velocity amplitude) on all spectral graphs presented here. All the vibration velocity spectrums of the casing of the microturbine were obtained during its stable operation, in other words – at constant power and at a constant rotational speed of the rotor. The performance of measurements at changing speeds would require the application of special signal analysis methods, used for measuring nonstationary states [20]. Moreover, if various measurement results were obtained under varying operating conditions, their comparison among themselves would be difficult.

The results presented in this part of the article were obtained during one of the first tests of the microturbine, which took place several hours after the first start-up. It can be stated that it was a brand new machine without any defects. The vibration of the machine was constantly monitored during these experiments. However, because of the page limit of the article, only selected measurement results (obtained at different rotational speeds) are presented. During these measurements, the rotational speed, power as well as thermodynamic parameters of the working medium's vapour were stable. Fig. 3 shows the vibration velocity spectrum obtained at the rotor speed of 9,300 rpm, while Fig. 4 and Fig. 5 demonstrate vibration velocity spectrums obtained at speeds of 18,060 rpm and 21,060 rpm, respectively.

On all the spectral graphs presented, we can observe one dominant vibration component, occurring at the frequency that corresponds to the rotational frequency of the rotor (the so-called synchronous vibrations). In the consecutive figures, these frequencies are as follows: 155 Hz, 301 Hz and 351 Hz. The vibration velocity amplitude increased as the rotational speed of the rotor increased; it was 0.20 mm/s, 0.36 mm/s and 0.52 mm/s. The constant increase in the vibration level is natural in the speed range analysed as it results from an increase in the centrifugal force (coming from the residual unbalance), which forces rotor vibrations in the transverse direction. The rotor of the tested microturbine is subcritical throughout the operating speed range because the resonant speed (corresponding to the lowest resonant frequency of the bending vibrations), obtained from numerical simulations, was about 130,000 rpm [30]. As a result, a gradual increase in the vibration level as the rotational speed increased was in accordance with our expectations and did not indicate a dynamic problem. In the re-

maining frequency range, there was also an increase in the vibration level at the lowest frequencies (up to about 20 Hz). However, these vibrations were not related to the operation of the microturbine and occurred even at the time when the rotor was not working. In the very low frequency range, vibrations of the construction of the test rig and of the foundation on which it was placed occurred (the floor is located in the laboratory on the first floor, whose ceiling is a lattice construction). The vibrations of these elements were induced, among other things, by the movement of people present in the laboratory and we were unable to eliminate them during the experiments. In addition, at rotational speeds of 18,060 rpm and 21,060 rpm, a slightly higher vibration level occurred at frequencies two times higher and two times lower than the rotational frequency; these are the components 2X and 1/2X. However, due to the very low vibration velocity amplitudes (lower than 0.05 mm/s), these components did not have a significant impact on the dynamic state of the machine.
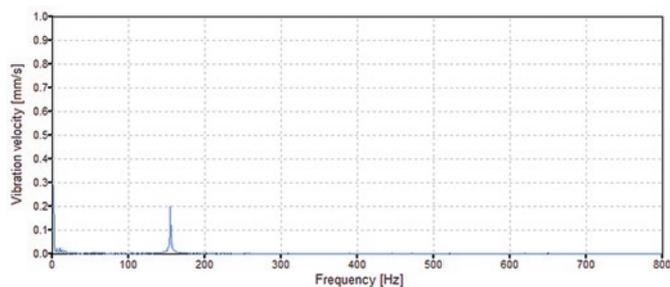
Fig. 3. The vibration velocity spectrum measured on the microturbine casing at a rotational speed of 9,300 rpm (155 Hz)
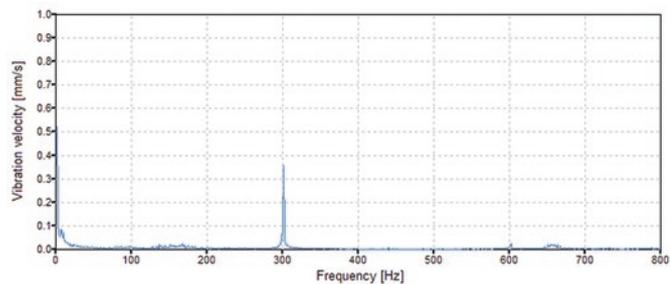
Fig. 4. The vibration velocity spectrum measured on the microturbine casing at a rotational speed of 18,060 rpm (301 Hz)
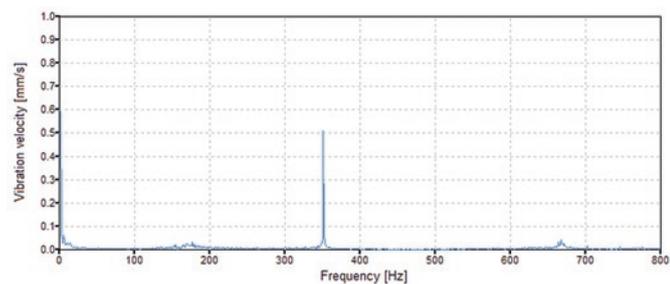
Fig. 5. The vibration velocity spectrum measured on the microturbine casing at a rotational speed of 21,060 rpm (351 Hz)

By evaluating the recorded vibration levels according to the relevant standards, we can affirm that the dynamic state of the tested microturbine was very good. According to the ISO 10816 standard, the overall vibration velocity amplitude (Vrms), measured on the casing of rotating machines with a nominal power up to 15 kW, should not exceed a value of 1.8 mm/s. If this requirement is met, a long-lasting operation is possible without any limitations. As for the machine discussed, the highest vibration velocity amplitude was only 0.52 mm/s and was recorded at a speed of 21,060 rpm. Although the overall vi-

bration level was slightly higher (0.71 mm/s), it was still lower than the maximum value allowed for newly commissioned machines.

Since the tested microturbine worked well across the full range of loads and rotational speeds, the results presented in this part of the article can be treated as reference values. They were obtained from the turbomachine whose technical condition did not raise any doubts. The results of these measurements can, therefore, serve as a reference point for further research or evaluations of the dynamic state of the machine after a certain period of operation. The vibration velocity spectrums obtained can also be useful for determining the symptoms of different types of defects.

3.2. Studies of the microturbine with an unbalanced rotor

The microturbine, after initial tests that proved its proper design parameters and its very good dynamic state, was subjected to further laboratory testing. The purpose of these tests was, among other things, to determine its operating characteristics (such as the output power or the temperature and pressure drops of the working medium). Vibration measurements were also performed. The purpose of the vibrodiagnostic research was to detect potential dynamic problems of the microturbine and the different types of defects that may have occurred due to the experimental nature of the ORC cogeneration system and also due to the fact that it had been tested under different conditions, even the rapidly changing ones [29].

The first symptoms, which indicated the deterioration of the dynamic performance of the machine, were observed after less than 100 hours of operation. It was disturbing to see an increase in the vibration level of the microturbine casing, which was particularly evident at high rotational speeds. A detailed analysis of recorded vibration velocity spectrums showed that apart from the synchronous component (1X), there were no other components on the graphs, however, the level of synchronous vibrations increased significantly. The vibration velocity amplitude was 0.74 mm/s at a speed of 20,520 rpm (Fig. 6) and increased to 0.87 mm/s at a speed of 21,000 rpm (Fig. 7). Compared to the reference value, the vibration level increased by about 67% at a similar rotational speed. Apart from the increased vibration level, there were no other signs that suggested that the microturbine malfunctioned.

To uncover the reason behind such an increase in the vibration level, a decision was made to disassemble the microturbine and conduct a visual inspection of its parts. Already at the beginning of the disassembly, after removing the cover of the casing at the non-drive end (NDE), it was found that the keep plate of the thrust bearing was covered with impurities, as shown in Fig. 8. The cavities in the keep plate that are visible on the photo are not a sign of damage as they were made intentionally when balancing the rotor. When continuing the disassembly of the microturbine, it turned out that a large part of the surface of the rotor was covered with impurities, which caused, among other things, an increase in its unbalance. The increased amplitude of the synchronous component (1X), observed during the vibration measurements, was a typical sign which indicated that the unbalance of the rotating system was too big.

To find the cause of the appearance of impurities on the rotor, the previous tests, which were carried out on the same test rig, were analysed. As this is a general-purpose test rig, it was previously used to study various subassemblies of the ORC system, including different types of circulation pumps. It turned out that the working medium of the ORC system was found to be contaminated with oil that got into the cycle as a result of the failure of one of the pumps tested. This was the membrane pump whose membranes (made of plastic) were not sufficiently resistant to long-lasting contact with the low-boiling medium. Due to the rupture of the membrane, oil from the the pump was flushed out to the ORC. Although the low-boiling medium was replaced in the ORC system after this incident, a significant amount

of oil remained inside the pipeline and other parts of the test rig (for example, in heat exchangers). In later tests, the oil mixed with the low-boiling medium entered the microturbine. When the microturbine ran at high temperatures, oil settled on its components. The surface of the rotor was affected by prolonged contact with the mixture of low-boiling medium and oil. After taking a look at Fig. 8, it becomes clear which part of the casing has been in contact with this mixture.
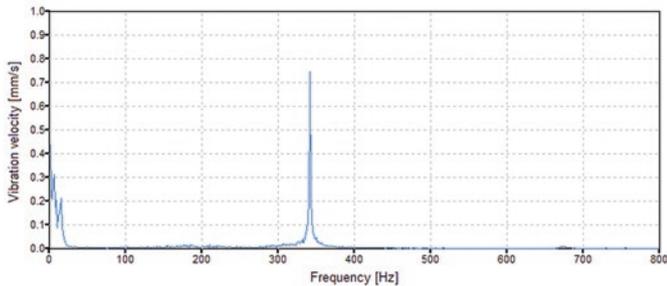
Fig. 6. *The vibration velocity spectrum of the microturbine with an unbalanced rotor, measured on the casing at a rotational speed of 20,520 rpm (342 Hz)*
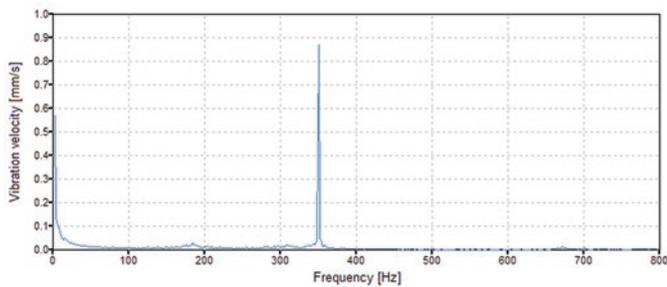
Fig. 7. *The vibration velocity spectrum of the microturbine with an unbalanced rotor, measured on the casing at a rotational speed of 21,000 rpm (350 Hz)*
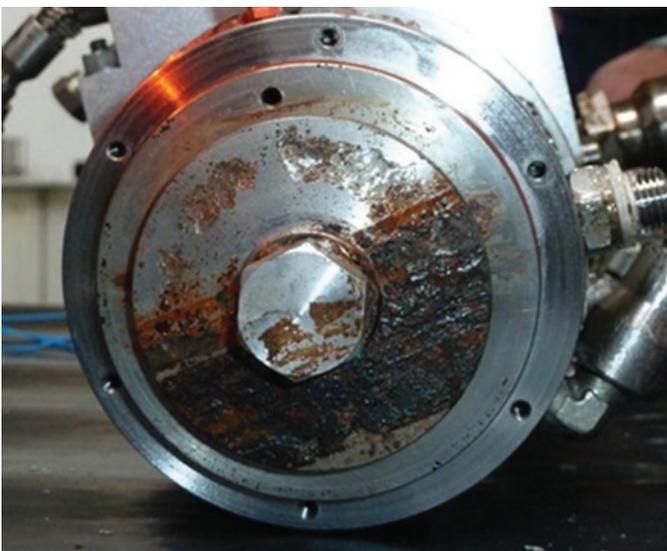
Fig. 8. *The bearing keep plate with the defect causing the rotor unbalance*

After the disassembly of the microturbine subassemblies, the parts underwent cleaning to remove oil deposits and impurities. The microturbine was restored to its initial technical condition. Prior to further testing, the entire ORC installation was washed and the low-boiling medium was filtered. The actions undertaken have made it possible to re-launch the test rig with the microturbine. Vibration measurements were conducted and their results confirmed the very good dynamic state of the machine. To sum up this part of the article, it can be added

that the deterioration of the dynamic state of the turbomachine under test was neither caused by a design mistake nor improper fabrication or assembly but was the result exclusively of inadequate operating conditions, namely, the microturbine was powered using the working medium mixed with oil.

3.3. Research on the microturbine with a malfunctioning bearing

The removal of the remaining oil from the microturbine and the ORC installation restored the test rig to its original state, thus allowing further investigation. Next signs of the microturbine malfunction appeared after one of the several-week-long idle periods. The microturbine was able to operate correctly but only at very low rotational speeds (up to about 6,000 rpm). At higher speeds, it was observed that apart from the 1X component, harmonic components such as 2X, 3X, 4X (and higher) appeared on the vibration velocity spectrums recorded on the casing. In addition, each of these components was not only present at one frequency value but also at the neighbouring ones. The amplitude of the 2X component was similar to that of the 1X component and the amplitudes of subsequent harmonics decreased gradually, as shown in Fig. 9. Despite the disturbing increase in the vibration level, the research was continued, increasing the rotor speed. At rotational speeds above 12,000 rpm, higher harmonics began to gradually disappear but the main component of the spectrum (1X), whose frequency corresponded to the rotational speed of the rotor, also began to appear at the neighbouring frequencies. The vibration spectrum became chaotic, as shown in Fig. 10. These types of spectrums are typical for rotating systems in which there is physical contact between rotating components and the casing or other non-rotating components. Since the vibration characteristic did not improve after several subsequent measurements, it was decided to disassemble the machine and check the technical condition of all its components.

During the disassembly of the microturbine, both the front and rear cover of the casing was removed, and the rotor was taken out. Visual inspection of the components revealed clear signs of wear of one of the gas thrust bearings (Fig. 11), indicating that it malfunctioned. This bearing was located at the free end of the shaft (see Fig. 1). Nearly half of the sliding surface showed signs of friction, which were the result of physical contact of the bearing with the surface of the keep plate. On closer inspection, it was found that 3 out of 10 supply holes were clogged. These holes are used to deliver the lubricating medium (in the form of low-boiling medium vapour) into the space between the sliding surfaces. Since the holes are small in diameter (only 0.4 mm), small particles of different sediments, from different parts of the installation, clogged them. The long downtime was detrimental to the microturbine because impurities accumulated in the supply chambers of the gas bearings. Due to the clogging of the holes, the amount of vapour delivered to the bearing lubrication gap decreased, resulting in a decrease in capacity. The axial force, transmitted by the shaft to the thrust bearing, increased as the flow rate and pressure of the vapour delivered to the microturbine blade system increased. This force was too high for the defective bearing, which resulted in the physical contact between two mating bearing surfaces. Under normal operating conditions, these surfaces are entirely separated by a lubricating film.

A visual inspection of all microturbine components showed that only the sliding surface of one of the thrust bearings was damaged. Since the keep plate was made of a much harder material, the damage only occurred on the surface of the bearing sleeve (made of bronze). Constant monitoring of the vibrations enabled early detection of this problem, so it was easy to repair the damage; the entire surface was smoothed by grinding. After the repair, the operation of the microturbine seemed normal and both the vibration velocity spectrum and the overall vibration level differed only slightly from the reference values.
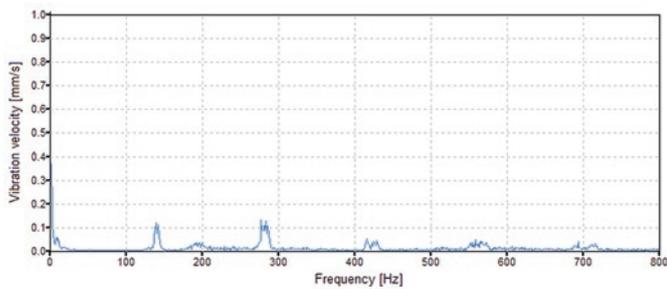
Fig. 9. *The vibration velocity spectrum of the microturbine with a damaged thrust bearing, measured on the casing at a rotational speed of 8,340 rpm (139 Hz)*
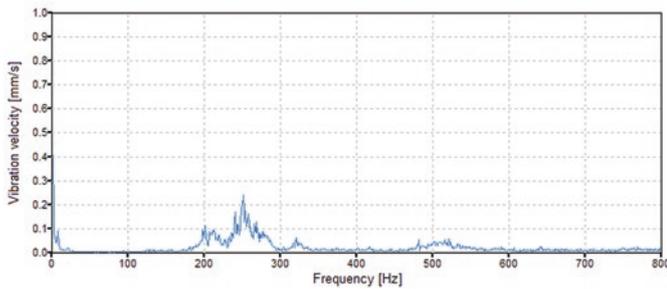
Fig. 10. *The vibration velocity spectrum of the microturbine with a damaged thrust bearing, measured on the casing at a rotational speed of 15,060 rpm (251 Hz)*
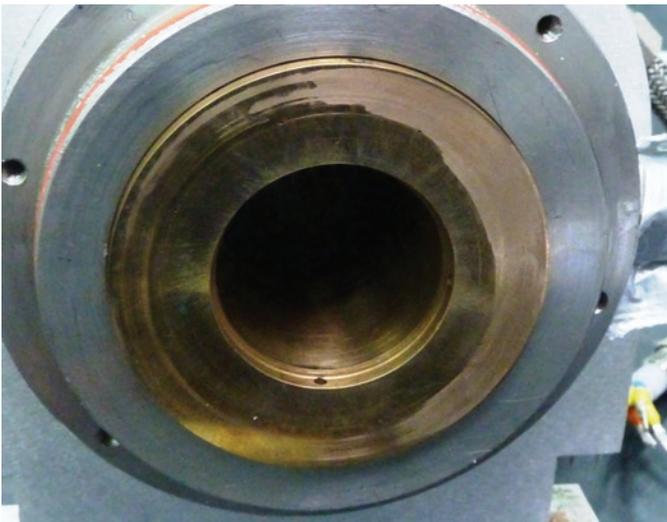
Fig. 11. *Gas thrust bearing with a damaged sliding surface*

3.4. Research on the microturbine with a bent shaft

This section describes another case of malfunctioning of the 2.5 kW ORC microturbine. It was observed that in addition to the synchronous component (1X), the vibration spectrum also included the harmonic component (2X) with a frequency twice as high as the current rotational frequency of the rotor. The amplitude of the 2X component was generally two times lower than that of the 1X component, regardless of the rotational speed. Two exemplary spectral graphs, showing such a distribution of vibration amplitudes, are in Fig. 12 and Fig. 13. The results demonstrated on these graphs were obtained during measurements at 11,280 rpm and 13,260 rpm. With regard to the second graph (Fig. 13), we can notice that in addition to the 2X component, the vibration spectrum also has a component with a frequency three times higher than the basic frequency. However, the

amplitude of the 3X component was much lower than the amplitudes of the 1X and 2X components and, therefore, had a negligible impact on the overall vibration level, on the basis of which the dynamic state of machines is evaluated.
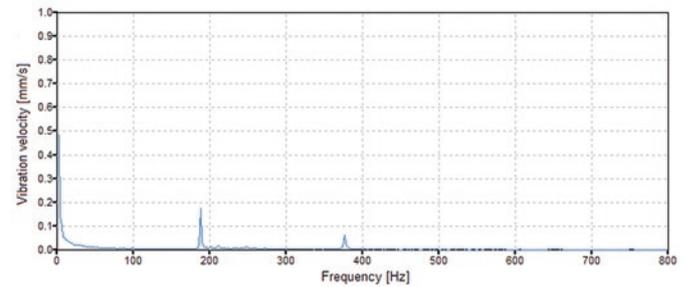
Fig. 12. *The vibration velocity spectrum of the microturbine with a bent shaft, measured on the casing at a rotational speed of 11,280 rpm (188 Hz)*
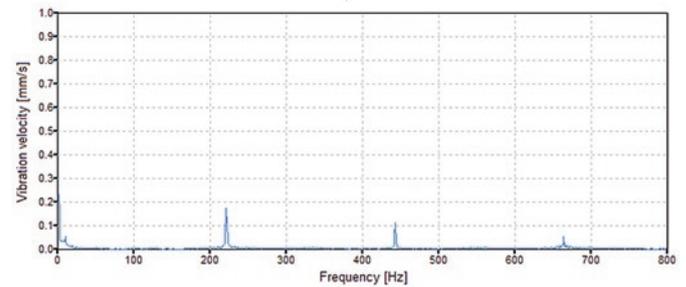
Fig. 13. *Vibration velocity spectrum of the microturbine with a bent shaft, measured on the casing at a rotational speed of 13,260 rpm (221 Hz)*

When the 2X component is present on a vibration spectrum graph and is present after changing the rotational speed, it usually means that either the shaft is bent or there is a misalignment of two mating shafts. Since the rotating machine discussed herein has only one shaft, it was suspected that the bent shaft was the main reason for the appearance of the 2X component. An analysis of the microturbine design, as well as its start-up and operating conditions, confirmed that the failure of the shaft was very likely. The inlet of the fresh vapour that powers the blade system of the microturbine is located only on one side of the casing (see Fig. 1), which results in the rotor not being uniformly heated. The rotor of this machine starts rotating only after there is an appropriate differential pressure between the vapour inlet and outlet. This means that it cannot be evenly heated during the initial start-up period. A similar situation occurs with radial gas bearings, which are powered through small-diameter holes. If the pressure of the lubricating medium is too low, the bearing journals cannot be lifted. This means that the supply holes in the lower parts of the bearings are blocked by the journals and vapour flows through the remaining holes. Only after the pressure increases, causing the journals to move towards the centres of the bearings, a similar amount of vapour starts flowing through all the supply holes. What aggravates the situation more is that two inlets of hot vapour which power the bearings are located on the same side of the casing. When starting the machine, this may cause thermal deformations as the casing is not evenly heated. Since the bearing sleeves are tightly mounted in the casing, its deformations also cause changes in the geometry of the bearing lubricating gaps. All this clearly shows that the microturbine's rotating system is susceptible to thermal deformations and that they may be the reason behind the appearance of diagnostic symptoms associated with a bent shaft.

A detailed study of this phenomenon showed that additional harmonic components (the clearly visible 2X component and the much lower 3X component) appeared mainly during the quick starts of the

microturbine and then disappeared after a few minutes of operation. When the casing, bearings and the rotor were heated over a longer period of time, this problem practically did not exist anymore. Therefore, in order to avoid a temporary deterioration of the dynamic performance, the settings of the test rig control system were changed so that the start of the microturbine always takes places after the temperature distribution is uniform.

4. Summary and conclusions

The results of vibrodiagnostic studies of the prototypical vapour microturbine with a maximum electric power of 2.5 kW have been discussed. The microturbine was designed for small ORC cogeneration systems, which can be used in single-family houses to produce heat and electricity. Experimental tests of the microturbine were performed under laboratory conditions, on the test rig that made it possible to simulate real operating conditions and apply the target working medium. Since the turbomachine tested had relatively low power and compact dimensions, it was possible to conduct research even after different types of defects of the rotating system had been detected. In the case of large steam turbines, such tests never take place because if there is a suspicion of serious damage to their bearings or rotor, the operation must be interrupted immediately. In addition, the costs of dismantling and repairing a large steam turbine are incommensurable. It was possible to carry out extensive research on the micro-power fluid-flow machine (despite the very high rotational speed – above 20,000 rpm), even in cases where its dynamic characteristics raised concerns. Until now, no research of this type, carried out on energy microturbines, has been presented in the scientific literature.

Based on the research carried out, it can be said that all the detected defects occurred due to improper operation, and in none of the cases were they due to faulty construction, improper fabrication or assembly. All the defects that caused the malfunction of the microturbine were detected using vibrodiagnostics. With regard to specific operating states of the machine, it was as follows:

- During the start-up and the initial period of operation, the microturbine was characterised by a very low vibration level and only the component corresponding to the rotational speed of the rotor (1X) was present on the vibration velocity spectrum. According to the ISO 10816 standard, the dynamic state of the tested machine was very good. The vibration level of the casing was typical for new machines, recently put into service.
- After the pump failure, the oil got mixed with the working medium of the ORC system and then entered the microturbine. As a result, sediments appeared on some parts of the rotor, causing, among other things, a significant unbalance of this component of the microturbine. During diagnostic measurements, this resulted in a considerable increase in the synchronous vibration level (by more than 60%); in other words, the 1X component increased significantly.
- In the case of the defective thrust bearing, in which a few supply holes were clogged, the vibration velocity spectrums became chaotic above certain rotational speeds, which may have been indicative of the occurrence of physical contact between the rotating and non-rotating components of the machine. When the speed increased above 6,000 rpm, higher harmonics appeared and dispersed on nearby frequencies. Then, above 12,000 rpm, an atypical and chaotic vibration distribution was observed near the synchronous component.
- The rotor deflection was the last detected defect of the microturbine. However, this posed a problem only during the first moments after start-up. The analysis showed that the problem was probably related to the uneven heating of the rotor and casing. This problem can be solved by careful planning the heating procedure of the machine before its start-up.

Since all the defects that appeared during operation of the microturbine were detected very quickly, no serious damage occurred. Therefore, the microturbine was restored into operation (without any operating limitations), in a relatively short time and with low additional costs. It should also be noted that a substantial increase in the vibration level occurred only in the case of the unbalanced rotor. Other defects were detected using vibration spectrum analysis. As for the malfunctioning gas bearing and the rotor deflection, the overall vibration level was low. Simple diagnostic methods, based solely on constant monitoring the vibration level, would not have been reliable in this case and the microturbine could suffer serious damage.

The defects and their diagnostic symptoms, detected during the laboratory tests, will be used to create a diagnostic system as it seems to be necessary with regard to the target application of the microturbine. The results of the experimental research presented in this article could be useful for all engineers and researchers involved in the maintenance and diagnostics of various types of energy microturbines, including high-speed ORC microturbines used in small cogeneration systems which have become increasingly popular in recent years.

References

1. Barella S, Bellogini M, Boniardi S, Cincera S. Failure analysis of a steam turbine rotor. Engineering Failure Analysis 2011; 18: 1511-1519, https://doi.org/10.1016/j.engfailanal.2011.05.006.
2. Barsali S, De Marco A, Giglioli R, Ludovici G, Possenti A. Dynamic modelling of biomass power plant using micro gas turbine. Renewable Energy 2015; 80: 806-818, https://doi.org/10.1016/j.renene.2015.02.064.
3. Beith R. (ed.), Small and micro combined heat and power (CHP) systems. Cambridge: Woodhed Publishing Limited, 2011, https://doi.org/10.1533/9780857092755.
4. Czmochowski J, Moczko P, Odyjas P, Pietrusiak D. Tests of rotary machines vibrations in steady and unsteady states on the basis of large diameter centrifugal fans. Eksploatacja i Niezawodnosc - Maintenance and Reliability 2014; 16(2): 211-216.
5. Dominiczak K, Rządkowski R, Radulski W, Szczepanik R. Online prediction of temperature and stress in steam turbine components using neural network. Journal of Engineering for Gas Turbines and Power 2016; 138: 052606-1, https://doi.org/10.1115/1.4031626.
6. Drescher U, Bruggemann D. Fluid selection for the Organic Rankine Cycle (ORC) in biomass power and heat plants. Applied Thermal Engineering 2007; 27(1): 223-228, https://doi.org/10.1016/j.applthermaleng.2006.04.024.
7. Efimov N, Papin V, Bezuglov R. Determination of rotor surfacing time for the vertical microturbine with axial gas-dynamic bearings. Procedia Engineering 2016; 150: 294-299, https://doi.org/10.1016/j.proeng.2016.07.006.

8. Hong D, Joo D, Woo B, Koo D, Ahn C. Unbalance Response Analysis and Experimental Validation of an Ultra High Speed Motor-Generator for Microturbine Generators Considering Balancing. Sensors 2014; 14: 16117-16127, https://doi.org/10.3390/s140916117.

9. Kaczmarczyk T, Żywica G, Ihnatowicz E. Vibroacoustic diagnostics of a radial microturbine and a scroll expander operating in the organic Rankine cycle installation. Journal of Vibration Engineering 2016; 18(6): 4130-4147, https://doi.org/10.21595/jve.2016.17167.

10. Kataoka T, Kishikawa T, Sakata S, Nakagawa T, Ishiguro J. Remote monitoring and failure diagnosis for a microturbine cogeneration system. ASME Turbo Expo 2007, Montreal (Canada), GT2007-27355, https://doi.org/10.1115/GT2007-27355.

11. Keshtkar H, Alimardani A, Abdi B. Optimization of rotor speed variations in microturbines. Energy Procedia 2011; 12: 789-798, https://doi.org/10.1016/j.egypro.2011.10.105.

12. Kiciński J, Żywica G. Steam microturbines in distributed cogeneration, Cham: Springer, 2014, https://doi.org/10.1007/978-3-319-12018-8.

13. Klonowicz P, Witanowski Ł, Jędrzejewski Ł. A turbine based domestic micro ORC system. Energy Procedia 2017; 129: 923-930, https://doi.org/10.1016/j.egypro.2017.09.112.

14. Kozanecka D, Kozanecki Z, Tkacz E, Łagodziński J. Experimental research of oil-free support systems to predict the high-speed rotor bearing dynamics. International Journal of Dynamics and Control 2015; 3(1): 9-16, https://doi.org/10.1007/s40435-014-0074-9.

15. Kozanecki Z, Łagodziński J. Magnetic thrust bearing for the ORC high - speed microturbine. Solid State Phenomena 2013; 198: 348-353, https://doi.org/10.4028/www.scientific.net/SSP.198.348.

16. Kubitz L, Rządkowski R, Gnesin V, Kolodyazhnaya L. Direct integration method in aeroelastic analysis of compressor and turbine rotor blades. Journal of Vibration Engineering & Technologies 2016; 4(1): 37-42.

17. Liu C, Jiang D, Chen J, Chen J. Torsional vibration and fatigue evaluation in repairing the worn shafting of the steam turbine. Engineering Failure Analysis 2012; 26: 1-11, https://doi.org/10.1016/j.engfailanal.2012.06.001.

18. Margo P, Luck R. Energetic and exergetic analysis of waste heat recovery from a microturbine using organic Rankine cycles. International Journal of Energy Research 2013; 37(8): 888-898, https://doi.org/10.1002/er.2891.

19. Otsu Y, Somaya K, Yoshimoto S. High-speed stability of a rigid rotor supported by aerostatic journal bearings with compound restrictors. Tribology International 2011; 44: 9-17, https://doi.org/10.1016/j.triboint.2010.09.007.

20. Pawlik P. Single-number statistical parameters in the assessment of the technical condition of machines operating under variable load. Eksploatacja i Niezawodnosc - Maintenance and Reliability 2019; 21(1): 164-169, https://doi.org/10.17531/ein.2019.1.19.

21. Peirs J, Reynaerts D, Verplaetsen F. A microturbine for electric power generation. Sensors and Actuators 2004; 113: 86-93, https://doi.org/10.1016/j.sna.2004.01.003.

22. Poursaeidi E, Mohammadi Arhani M. Failure investigation of an auxiliary steam turbine. Engineering Failure Analysis 2010; 17: 1328-1336, https://doi.org/10.1016/j.engfailanal.2010.03.006.

23. Poursaeidi E, Taheri M, Farhangi A. Non-uniform temperature distribution of turbine casing and its effect on turbine casing distortion. Applied Thermal Engineering 2014, 71: 433-444, https://doi.org/10.1016/j.applthermaleng.2014.07.019.

24. Wang W, Buhl P, Klenk A, Liu Y, The effect of in-service steam temperature transients on the damage behavior of a steam turbine rotor. International Journal of Fatigue 2016; 87: 471-483, https://doi.org/10.1016/j.ijfatigue.2016.02.040.

25. Witek L, Orkisz M, Wygonik P, Musili D, Kowalski T. Fracture analysis of a turbine casing. Engineering Failure Analysis 2011; 18: 914-923, https://doi.org/10.1016/j.engfailanal.2010.11.005.

26. Zhang D, Xie Y, Feng Z. An investigation on dynamic characteristics of a high speed rotor with complex structure for microturbine test rig. ASME Turbo Expo 2008, Berlin (Germany), GT2008-50411, https://doi.org/10.1115/GT2008-50411.

27. Ziegler D, Puccinelli M, Bergallo M, Picasso A. Investigation of turbine blade failure in a thermal power plant. Case Studies in Engineering Failure Analysis 2013; 1: 192-199, https://doi.org/10.1016/j.csefa.2013.07.002.

28. Żywica G, Bagiński P. Investigation of gas foil bearings with an adaptive and non-linear structure. Acta Mechanica et Automatica 2019; 13(1): 5-10, https://doi.org/10.2478/ama-2019-0001.

29. Żywica G, Kaczmarczyk T, Ihnatowicz E, Turzyński T. Experimental investigation of the domestic CHP ORC system in transient operating conditions. Energy Procedia 2017; 129: 637-643, https://doi.org/10.1016/j.egypro.2017.09.123.

30. Żywica G, Kiciński J. The influence of selected design and operating parameters on the dynamics of the steam micro-turbine. Open Engineering 2015; 5: 385-398, https://doi.org/10.1515/eng-2015-0038.

Grzegorz ŻYWICA
Tomasz Z. KACZMARCZYK
Department of Turbine Dynamics and Diagnostics
Institute of Fluid Flow Machinery, Polish Academy of Sciences
Fiszera 14 str., 80-231 Gdansk, Poland

E-mails: gzywica@imp.gda.pl, tkaczmarczyk@imp.gda.pl